



J R C T E C H N I C A L R E P O R T S

External quality control of SPOT6 orthoimagery

Geometric benchmarking over Maussane test site for positional
accuracy assessment

J. Grazzini
P. Astrand

2013

Report EUR 26103 EN

European Commission
Joint Research Centre
Institute for Environment and Sustainability

Contact information

P. Astrand

Address: Joint Research Centre, Via Enrico Fermi 2749, TP 266, 21027 Ispra (VA), Italy

E-mail: par-johan.astrand@jrc.ec.europa.eu

Tel.: +39 0332 78 6215

Fax: +39 0332 78 6325

<http://cidportal.jrc.ec.europa.eu/> <http://www.jrc.ec.europa.eu/>

This publication is a Reference Report by the Joint Research Centre of the European Commission.

Legal Notice

Neither the European Commission nor any person acting on behalf of the Commission is responsible for the use which might be made of this publication.

Europe Direct is a service to help you find answers to your questions about the European Union Freephone number (*): 00 800 6 7 8 9 10 11

(*): Certain mobile telephone operators do not allow access to 00 800 numbers or these calls may be billed.

A great deal of additional information on the European Union is available on the Internet. It can be accessed through the Europa server <http://europa.eu/>.

JRC 82314

EUR 26103 EN

ISBN 978-92-79-32543-4

ISSN 1831-9424

Contents

Abstract		ii
Acknowledgments		iii
1 Introduction	4	
2 SPOT6 sensor	5	
3 Benchmarking methodology	7	
3.1 Test objectives	7	
3.2 Test workflow design	8	
4 Input data	9	
4.1 Selection of AOI over Maussane test site	9	
4.2 Primary images	13	
4.3 Ancillary data	13	
5 Orthorectification process	14	
5.1 Ancillary modeling data preparation	14	
5.2 Remarks regarding the orthorectification process	15	
6 External geometric quality control	16	
6.1 Auxiliary validating data preparation	17	
6.2 Results and discussion	18	
7 Conclusion	26	
Annex		28
References		30
List of Figures	xxxii	

List of Tables xxxiii

Abstract

The main objective of the present study is to assess whether SPOT6 sensor can be qualified for Control with Remote Sensing (CwRS) programme, in Common Agriculture Policy (CAP). The benchmarking presented herein aims at evaluating the usability of SPOT6 for the CAP checks through an estimation of its geometric (positional) accuracy, as well as measuring the influence of different factors (viewing angle, number of GCPs, software implementation) on this accuracy. For that purpose, the External Quality Control of SPOT6 orthoimagery conforms to the standard method developed by JRC and follows a procedure already adopted in the validation of previous high (HR) and very-high resolution (VHR) products.

Following the results of this benchmarking, it is asserted that SPOT6 sensor can be used in the various CwRS program with the following technical specifications:

- the multispectral orthoimagery can be used in HR CwRS with a planimetric accuracy – expressed as the misregistration in both Easting and Northing directions – below 8m, provided that 3 GCPs at least are used in the (RPC) orthorectification model;
- the panchromatic orthoimagery, as well as the commercialised pansharpened orthoproducts, can be considered for use in backup VHR CwRS with a planimetric accuracy below 4m, with the same condition as before.

This assertion may be further refined with later in-depth analysis.

Acknowledgments

The authors would like to thank F. Ranera (Astrium) for generating the orthoimagery considered in the benchmarking presented in this report. They also acknowledge his various

comments regarding the outcomes of the benchmarking, and his numerous suggestions throughout the study as well as for the redaction of the final document.

1 Introduction

The EU standard for the orthoimagery to be used for the purpose of Common Agriculture Policy (CAP) checks requires appropriate quality of the input data, as well as the quality assessment of the final orthoimagery [1]. Within this context, the objective of the current study is to perform an initial quality assessment of the geometric capabilities of the newly launched SPOT6 satellite.

In order to fulfill Control with Remote Sensing (CwRS) requirements [2, 3], it has been proposed to assess the geometric (planimetric) accuracy of **SPOT6 products** commercially distributed by Astrium. Hence, the following spectral combinations (see Figure 1) are considered:

- bundle products: Panchromatic (PAN: 1.5m spatial resolution) and Multispectral (MSP: 6m) images, whose processing level is the closest to the data acquired by the sensor, and
- Pansharpened products (PSH: 1.5m) that consist of georeferenced and orthorectified images using in-house Astrium Reference3D dataset.

The geometric validation of these products is based on the External Quality Control (EQC) of the orthoimagery and follows strict guidelines enounced by JRC in the so-called "**Guidelines for Best Practice and Quality Checking of Ortho Imagery**" [4]. In practice, the EQC aims at checking the registration error as the RMSE in both Easting and Northing directions, also denoted $RMSE_{1D}$. Namely, considering the different processing levels of the products distributed by the image provider, the following operations are performed:

- [1.i] the **testing of primary PAN and PSH imagery for use of the sensor in backup VHR CwRS** – in which a $RMSE_{1D}$ of twice the Ground Sampling Distance (GSD) of the products is usually accepted [3], hence $2 \times GSD = 3m$ here – through the benchmarking of derived orthoproducts,
- [1.ii] the **testing of primary MSP imagery** (see for instance Figure 2) **for use in HR CwRS** – in which a $RMSE_{1D}$ of 1.5 times the GSD ('thumb rule') is often expected [3], hence $1.5 \times GSD = 9m$ here – also through the benchmarking of derived orthoproducts,
- [1.iii] the **direct testing of ready orthorectified PSH products for use in backup VHR CwRS as well** (see Figure 3).

The rest of the report is organised as follows. Next Section introduces the SPOT6 sensor and its main characteristics. Section 3 presents the adopted benchmarking methodology and the processing workflow. Section 4 describes the primary imagery assessed for validation, and all other input data used for that purpose, while Section 5 succinctly presents the

2. SPOT6 sensor

orthorectification process in relation with the available input data. The results of the EQC are presented and discussed in Section 6. Final conclusions and statements regarding SPOT6 geometric assessment are drawn in Section 7.

2 SPOT6 sensor

SPOT6 sensor secures mission continuity of the SPOT series as it will operate in a constellation with SPOT7 sensor (when this latter will be launched). The main sensor properties are summarized in Table 1. The reader is also referred to the documentation released by the image provider for further information¹.

SPOT takes benefits from the high agility of the satellite to offer data collection capabilities suitable to serve cartographic and monitoring applications. In terms of images collection, SPOT6 sensor enables in standard mode (single pass):

- the acquisition of North-South long strip of up to 600km length,
- the collection of contiguous image segments along one orbit; this provides capability to cover areas of more than $120 \times 120km^2$ or $60 \times 180km^2$.
- quick moves from one scene to another along an orbit,
- corridor acquisitions – non North-South oriented – for covering certain areas in a customised way (*e.g.* riverbed, borders).

This provides a high efficiency to complete, in the shortest time, global data coverage over a large area of interest, allow acquisition conflicts avoidance and makes possible the collection of number of distant targets in a given geographical area in a single pass. In addition, the satellite allows to collect stereo pairs or triplets of images (from a single pass along one orbit) over areas of interest with viewing angles between two consecutive images separated with 15° or 20° with B/H ratio between 0.27 and 0.4.

Mission characteristics	
number of satellites	2: SPOT6 and SPOT7.
launch	SPOT6: September 12th, 2012 – SPOT7: Q1, 2014.
mission lifetime	Minimal: 10 years.
Orbital elements	
type	Sun-synchronous, 10:00 AM local time at descending node.
altitude	694km.

¹ See also image provider's website <http://www.astrium-geo.com/en/147-spot-6-7/>. ² Depends on the latitude of the area of interest.

period	98.79mn.
cycle	26 days.
revisit frequency	1 day with SPOT6 and SPOT7 operating simultaneously; between 1 and 3 days with only one satellite in operation ² .
Instruments properties	
optical system	One instrument made of 2 identical Korsch telescopes, each with a 200mm aperture, delivering the expected swath.
spectral resolution	PAN: BW=[0.450 - 0.745] μ m (black and white); MS bands: B=[0.450 - 0.520] μ m (blue), G=[0.530 - 0.590] μ m (green), R=[0.625 - 0.695] μ m (red), NIR=[0.760 - 0.890] μ m (near-infrared). The 5 bands are always acquired simultaneously.
detectors	PAN array assembly: 28000 pixels; MS array assembly: 4 \times 7000 (28000 in cross-track) pixels - each pixel having a size of 13 μ m.
spatial resolution	PAN: 1.5m; MS: 6.0m.
swath width	60km at nadir.
dynamic range per pixel	12 bits per pixel.
viewing angle	Standard: $\pm 30^\circ$ in roll; maximum: $\pm 45^\circ$ in roll.
pointing agility	Control Moment Gyroscopes allowing quick maneuvers in all directions for targeting several areas of interest on the same pass (30 $^\circ$ in 14s, including stabilization time).
acquisition capability	Up to 6.10 ⁶ km ² daily with SPOT6 and SPOT7 when operating simultaneously.
stereo capability	Fore and aft mode; single pass stereo and tri-stereo.
instrument TM link rate	X-band channel, rate of 300 Mbits/s.
onboard storage	1 Tbits end of life (Solid State Mass Memory).

Table 1: Main characteristics of SPOT system. Orbital elements and instruments properties¹.

The delivered products are:

- primary for mono, stereo and tristereo acquisitions as close to the original sensing conditions as possible (as little processing as possible),
- ortho rectified automatically where data from the geocoded database Reference3D (*a.k.a* Elevation30) are available ², with the following geolocation accuracy

specification (also given by the image provider):

² See <http://www.astrium-geo.com/en/2788-reference3d-your-geographic-reference-system>.

- 35m CE90 without GCP within a 30 ° viewing angle cone³,
- 10m CE90 for ortho products where Astrium in-house Reference3D is available⁴.

3. Benchmarking methodology

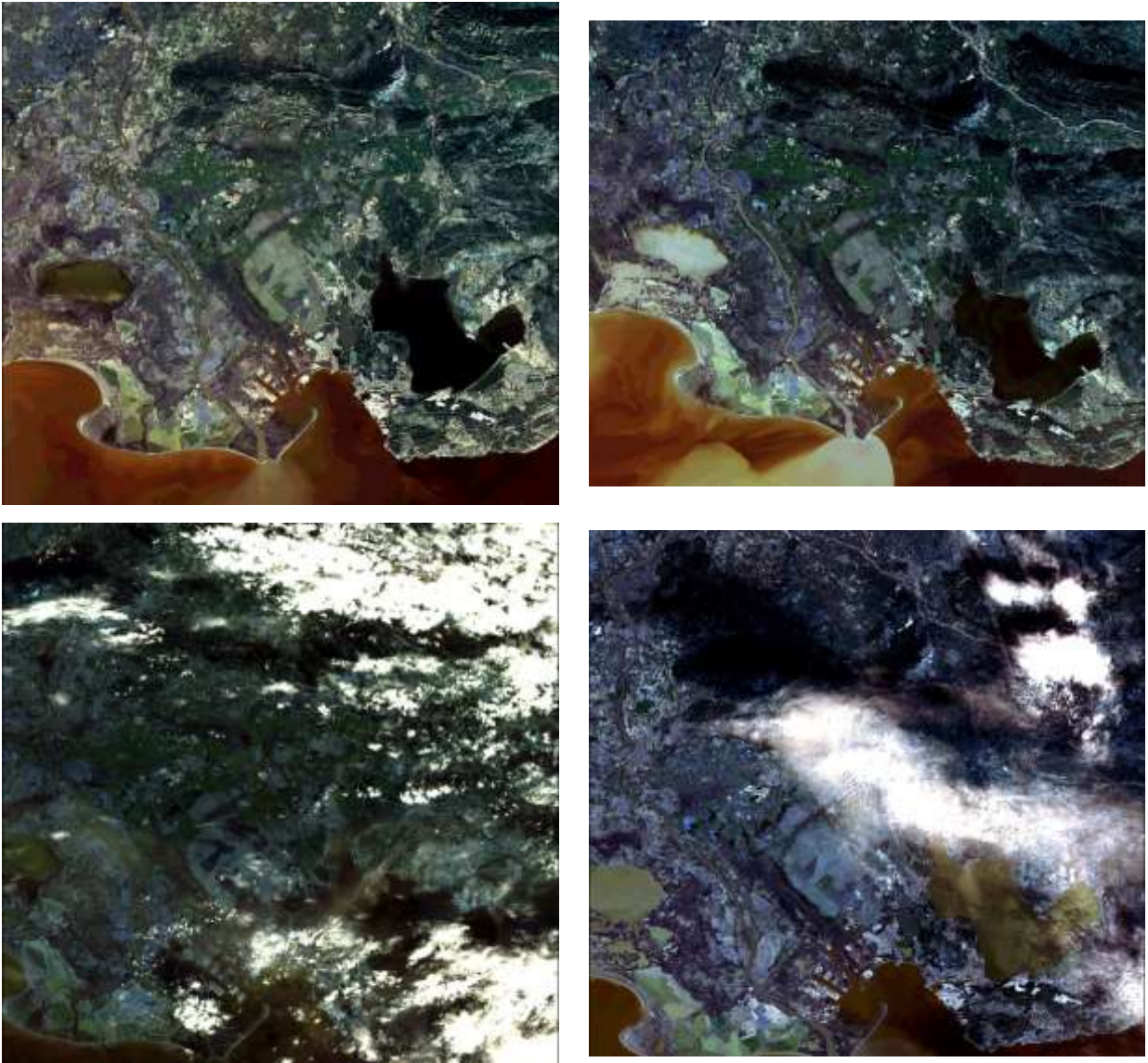


Figure 1: Examples of pansharpened SPOT6 acquisitions over Southern France. Images made available by Astrium for the preparation of the benchmarking. Top: cloud free 22 ° (left) and 27 °

³ Notice that this could (should) be assessed during the benchmarking by checking products orthorectified without the use of any GCP (*e.g.* see Pléiades study of [5]); the present analysis does however not provide such assessment.

⁴ According to Astrium, Reference3D orthoimages – derived from a uniform gridded DTED level 2 DEM

(right) primary products (see further description in Section 4.2). Bottom: some close-to-nadir acquisitions not considered in this study because of heavy cloud cover.

3 Benchmarking methodology

3.1 Test objectives

It is well known that the planimetric accuracy $RMSE_{1D}$ of the orthoimagery is sensitive to various influencing factors [6, 7]. As claimed in previous benchmarking/validation campaigns [8, 5], it is believed that having a strict control on the reference data and a sufficient

obtained through automatic correlation of SPOT HRS stereopairs – can provide ground control points accurate enough to ensure GPS compatibility: 10m CE90 (or 7m RMS).

priority ID	primary products	channels	# GCP	type	SW suites (RPC)	#ortho products	total #
1		PAN	3 and 4	'located'	ERDAS PCI Envi PCI	8	
5			1 and 5	'located'			
2	-13/11/12				Envi ERDAS, PCI, Envi		
3							
		MS				10	
6	.		3 and 4	'derived'	PCI		22
			3 and 4				
			1 and 5				
			3 and 4				
			1 and 5				
4	21	PSH		'derived'	PCI	4	
7							
.	4° -2/03/13	22
.							
.							
.	22° -20/11/12	22
.							
							66

Table 2: Benchmarked ortho products: proposed definition. In total, around 70 products (66 above plus 3 Reference3D PSH orthoimages) are produced for the proposed benchmarking. In terms of production, high priority was given to the above red shaded products; hence, notice that the production of orthoimages by Astrium first focused on the generation of [3,4]-GCPs based products.

proven quality, the results of the orthorectification are mainly influenced by the accuracy of the input data and the reliability of the geometrical model, and not by external factors. Hence, the scope of the benchmarking performed during operations [1.i] and [1.ii] comprises the following components:

- 3 primary images of different viewing angles are considered.
- The orthocorrection is performed on three independent image processing platforms: ERDAS, Envi, PCI providing distinct implementations of RPC models. This process is operated by the image provider.
- Concerning the Ground Control Points (GCP) used for modeling the orthocorrection process, 4 different input configurations are considered, with 1, 3, 4 and 5 GCP(s) respectively, with different testing purposes however. Exactly the same set of CPs is used for the generation of the various orthorectified products on the different software platforms.
- A single highly accurate raster Digital Elevation Model (DEM) is used.
- Well-defined ICPs with precision at least as accurate as that of the GCPs is considered for the evaluation of image correction performance.

To perform operation [1.iii], the set of ICPs used for validation is then the same as that mentioned above.

3.2 Test workflow design

The reader is referred to [5, Figure 1, Section 3] for a clear representation of the different task assignments through the test workflow. The bundle (PAN and MSP) products are validated using, for modeling the orthocorrection process, one unique set of GCPs estimated over the

PAN images and provided by JRC. In particular, the tested MSP ortho products are generated using:

- a '*derived*' set of GCPs obtained through a downsampling of the corresponding PAN GCPs locations,
- in addition, another native set of '*located*' GCPs, independently and directly estimated over the MSP images.

Concerning the processed ortho products and their evaluation, it means that priority is given in a first stage to:

[3.i] the PAN and MSP images generated using the RPC models implemented in the different available softwares (ERDAS, Enviand PCI, *cf.* Section 3.1 above), and input configurations with 3 and 4 '*derived*' GCPs (estimated in the PAN images) as those configurations are most oftenly considered for orthorectification,

[3.ii] the so-called Reference3D PSH images commercialised by Astrium, for a primary assessment, and in a second stage to:

[3.iii] the PAN and MSP images generated using PCI software with 1 and 5 '*derived*' GCPs (see above explanation),

[3.iv] the PSH images generated using PCI software with 1, 3, 4 and 5 GCPs,

[3.v] the MSP images generated using Envi software with '*located*' GCPs (estimated directly in the MSP images),

for a further characterisation and validation. The final list of benchmark products (with their respective priorities) is given in Table 2. Conclusions are drawn from the the different sets of ortho products and given in Section 7.

4 Input data

For the various test cases to be elaborated, it is required to use in input (*i*) a set of primary raw images acquired with different viewing angles over a well-known area, and (*ii*) a set of well-defined ancillary data covering that same area: DEM and GCPs. The input data used in the benchmarking are presented in this section.

4.1 Selection of AOI over Maussane test site

The test site of Maussane, located in France, has been selected for benchmarking by JRC. That site has been used in previous HR [9, 10] and VHR [11, 5] quality assessments, as for the following reasons:

- it presents a variety of agricultural condition typical for the EU, as well as urban settlements and water bodies,

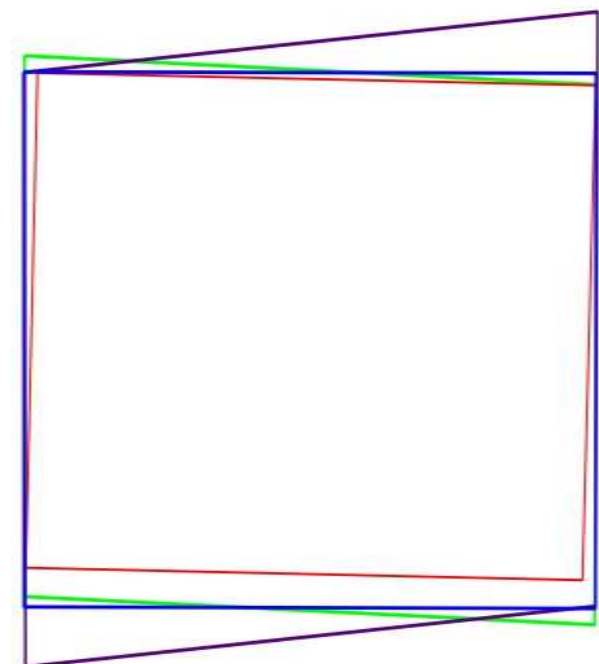


Figure 2: SPOT6 MSP (multispectral) products over Maussane test site and corresponding footprints. From top to bottom, from left to right: cloud free 4°, 22° and 27° primary products; corresponding footprints in EPSG 32631 reference system: blue, green and purple frameboxes resp. On this last figure, the 19×18km² Maussane AOI selected for geometric benchmarking is also represented as a red framebox. To be validated through operation [1.ii].



Figure 3: SPOT6 Reference3D PSH (pansharpened) orthoimagery over Maussane test site. From top to bottom, from left to right: 4°, 22° and 27° PSH delivered together with the MSP images of Figure 2. To be validated through operation [1.iii].

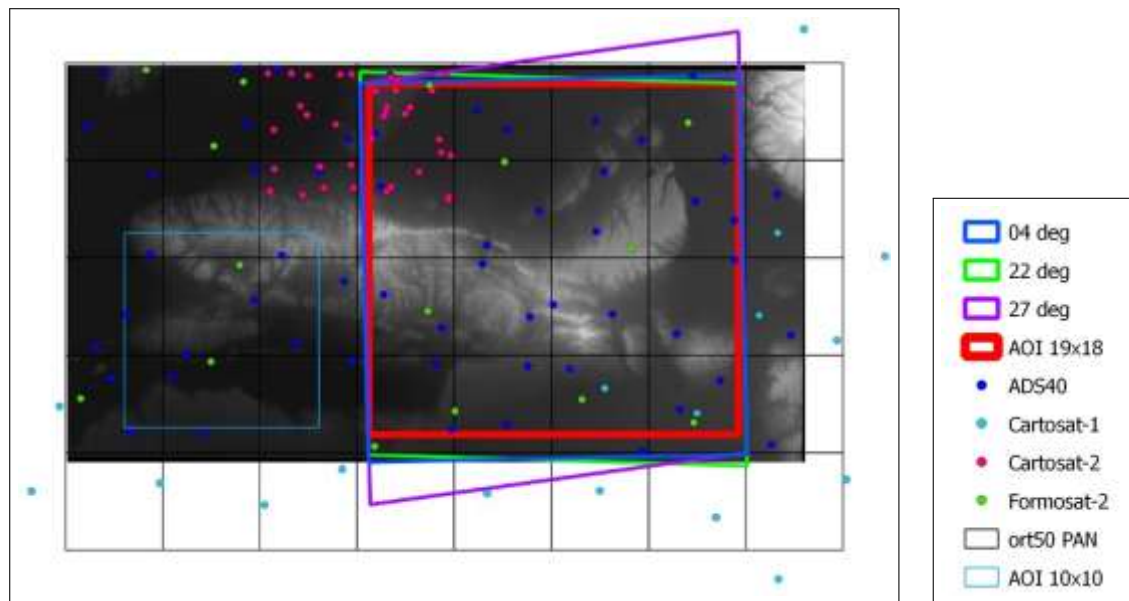


Figure 4: Maussane test site and related available JRC ancillary data: DEM and CPs. The ADS40 DEM covering a large extent ($\approx 35 \times 20\text{km}^2$) over Maussane area is displayed as a background grayscale layer (the brighter a pixel, the higher the elevation at that point). Over that same area, 4 datasets of CPs are retrieved from previous campaigns [12] and represented as coloured dots (\bullet) on the figure. The footprints of the SPOT6 acquisitions are represented as coloured frames (see also Figure 2). The $19 \times 18\text{km}^2$ AOI selected for SPOT6 validation is displayed as a bold red frame; note also that, for comparison, the $10 \times 10\text{km}^2$ AOI considered in previous Pléiades benchmarking [5] is displayed as a light blue frame. The grid used in ADS40 coverage is represented as well (so-called ort50 PAN). See legend and text for further description.

- it contains a low mountain massif (650m above sea level) mainly covered by forest, surrounded by agricultural areas.

In addition, it offers sufficient ancillary and reference data (GCPs, DEM) with a validated quality [12]. Following early acquisitions provided by Astrium (22° and 27° off-nadir viewing angles) and considering the available data (DEM and GCPs appropriate for HR/VHR validation), the AOI for geometric benchmarking is identified as a small rectangular subscene over Maussane site (see Figure 4):

- covering an extent of $19 \times 18\text{km}^2$ (East \times North) with UL corner at position (648800 E, 4854500 N) in EPSG 32631 (UTM - zone 310 N - ellipsoid WGS84) reference system⁵,

⁵ The UL corner's location in Geographic Lat/Lon coordinates is: DMS=(43.82859505 E, 4.85062756 N), or equivalently DEG=($43^\circ 49'42.94''$ E, $4^\circ 51'2.26''$ N).

- with rather dense coverage by existing CPs datasets and full coverage by desired DEM (see Section 4.3).

4.2 Primary images

As for the year 2013, 3 datasets (bundle: PAN and MSP; PSH) over the selected Maussane AOI have been acquired by SPOT6 for geometric benchmarking (see for instance Figure 2: MSP, and Figure 3: PSH):

- on 13/11/12 with viewing (off-nadir) angle around 27° ,
- on 20/11/12 with viewing angle around 22° ,
- on 2/03/13 with viewing angle around 4° ,

that is to say, all available input images were acquired during the winter season (with little to insufficient radiometric information).

4.3 Ancillary data

Control Points (simply denoted CPs) serve for the orthorectification of the images and the geometric quality validation of the derived orthoimages, provided the fulfilment of the accuracy requirements of JRC guidelines [4, Section 7.1]:

"GCPs [and ICPs] should be at least 3 times (5 times recommended) more precise than the target [accuracy] specification for the ortho⁶."

CPs over Maussane test site are retrieved from already existing datasets of GPS measurements performed during previous JRC campaigns [12] (see Figure 4):

1. CPs from ADS40 collection⁷ [12, Section 4],
2. CPs used in Cartosat-1 [12, Section 6] and Cartosat-2 [12, Section 8] validations,
3. CPs used in Formosat-2 project [12, Section 7].

The reader is also referred to [13, 14] for further information regarding the considered CPs databases.

A high-resolution/high-precision raster DEM with ellipsoidal heights is used for both HR and VHR benchmarking (see Figure 4):

- spatial resolution (grid size) of $2 \times 2m$,

⁶ Note that even though the accuracy of SPOT6 HR (resp. backup VHR) imagery is targeted to a RMSE of 9m (resp. 3m), the ancillary data used herein are that of VHR imagery (with target RMSE of 2.5m).

⁷ The ADS40 collection was also used in previous VHR validations, e.g. Pléiades accuracy assessment [5].

- vertical (height) accuracy of $RMSE_z \leq 0.6m$.

This DEM was produced from digital airborne stereo image pairs (Leica Geosystems) of GSD of 50cm in the frame of ADS40 project [12]. From that DEM, a subset is extracted so that a 400m-wider scope area than Maussane AOI is enclosed in the DEM AOI (see buffer around AOI, Figure 5). Within the context of SPOT6 validation (see specifications in Section 2), this DEM meets the requirements of JRC guidelines for orthorectification [4,

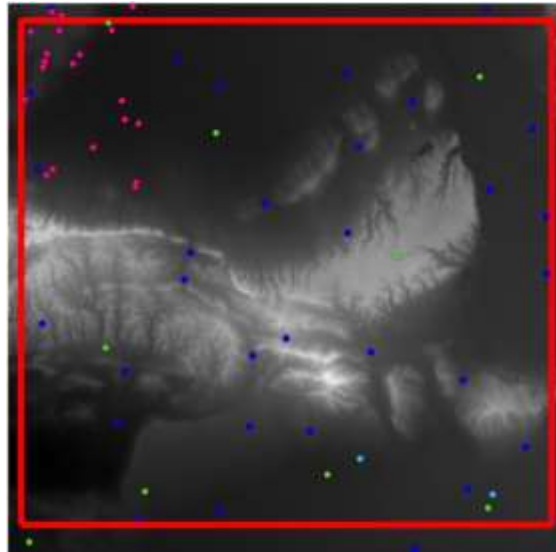


Figure 5: Available JRC ancillary data over Maussane AOI: DEM. Detail from Figure 4. The selected AOI is covered by the ADS40 DEM.

p.15]:

grid spacing \leftrightarrow "5 to 20 times of the orthophoto pixel size depending on the terrain flatness",
DEM accuracy \leftrightarrow "2 \times planimetric RMSE required".

5 Orthorectification process

This section outlines the orthorectification preparation – using different input data – for benchmarking, from the perspective of checking the final geometric quality of the output orthoproduct.

5.1 Ancillary modeling data preparation

In total, 5 GCPs are selected and used in different spatial configurations for benchmarking the various PAN, MSP ('derived' approach) and PSH products: see Figure 6. These GCPs are

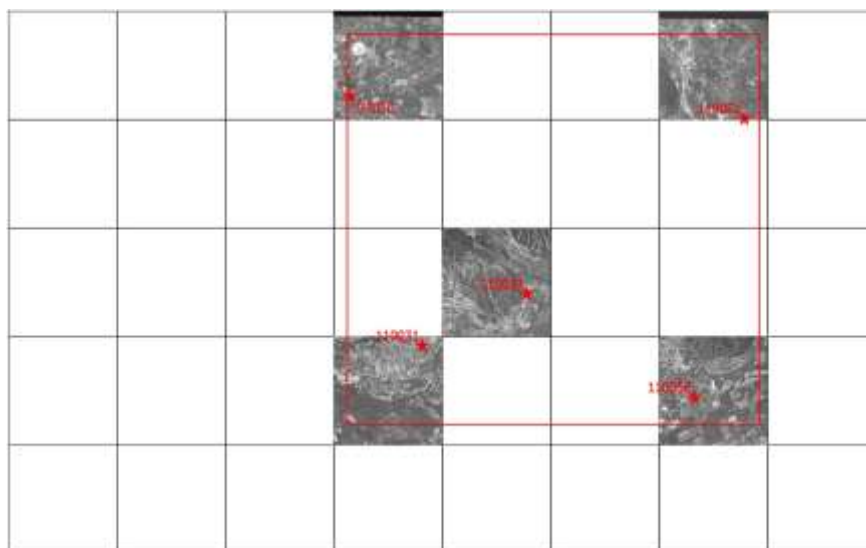
extracted from 2 of the prior mentioned CPs datasets (see Section 4.3 and Tables 8 and 9 in Annex A), namely:

- 1 GCP is taken from Cartosat-2 project database,
- 4 GCPs are taken from the ADS40 collection.

As mentioned in Section 4.3, the ortho-guideline requirements are met when considering the properties of the CPs datasets, as for the positional accuracy $RMSE_{1D}$:

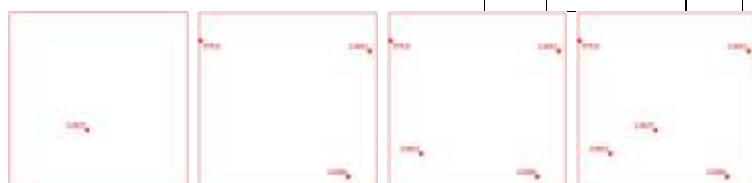
- with ADS40 CPs, $RMSE_{1D}[\text{East}] < 5\text{cm}$ and $RMSE_{1D}[\text{North}] = 10\text{cm}$,
- with Cartosat-2 CPs, $RMSE_{1D}[\text{East}] = 0.90\text{m}$ and $RMSE_{1D}[\text{North}] = 0.80\text{m}$,

5. Orthorectification process



(a) All 5 input GCPs used in orthorectification are identified in aerial images of the ADS40 dataset (PAN at 0.5m resolution) [14], and located in SPOT6 PAN and MSP images through visual position matching [6].

#	ID	GCPs							
		1	3	4	5				
1	110037		√	√	√				√
2	G7010		√	√	√				√
3	110051		√	√	√				
4	110056				√	√			
5	110031								



(b) Left: GCPs selection in primary raw images for the generation of the ortho-products. Right: GCPs (red star F) spatial configuration for the 22° and 27° images; from left to right: 1, 3, 4 and 5 GCP(s) selected.

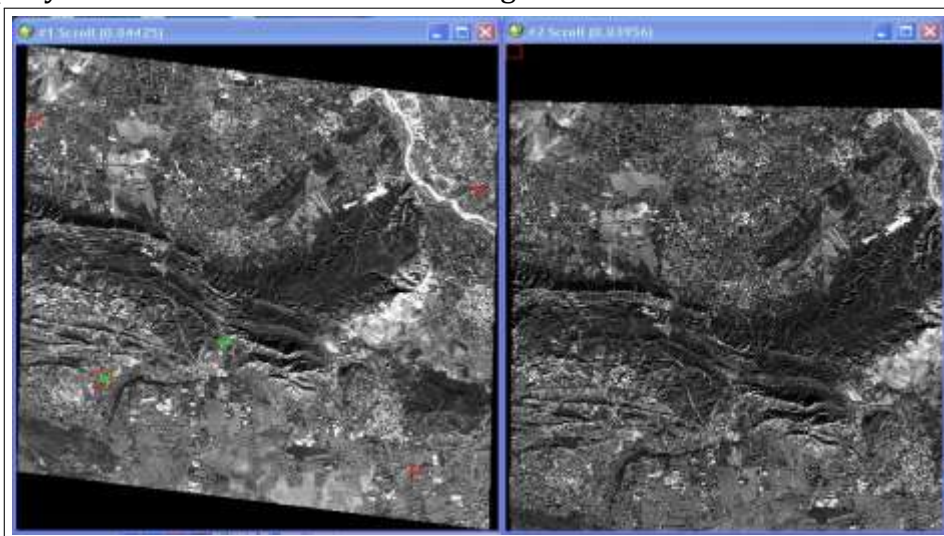
Figure 6: GCPs selection: ground and image identification; configuration.

and, as for the vertical accuracy, $RMSE_z$ is at least of 1m [12].

In practice, the (RPC based) orthorectification [15] of the PAN, MSP and PSH data is operated by the image/software providers. All GCPs are identically chosen for each software respective test in order to ensure the consistency of the software performance test. As stated before, 'located' and 'derived' positions are considered when correcting the MSP imagery (see Table 10 in Annex A).

5.2 Remarks regarding the orthorectification process

- Most of the remarks mentioned in [5, Sections 4.3 and 5.3] relevant to the correction of Pléiades imagery also apply to the correction of SPOT6 imagery, as the same sets of ancillary data are used herein. In particular, notice the fact that the DEM considered is a DSM and not a DTM (hence, its influence on the orthorectification accuracy should be tested), plus the fact that Control Points (GCPs, but ICPs as well, see next Section) should be defined in-situ following a prior analysis of the raw primary images.
- Some issues when orthorectifying images with the version of Envi software considered in this study were reported. Indeed, when performing the ortho-rectification, a pixel size of the ortho product is proposed by default by the software. However, if this pixel size is modified, a part of the image is missing. In our case, the output orthorectified image was missing the South-East part of the AOI (see Figure 7) as the size of the pixel was modified to fit to SPOT6 ortho specification; moreover, the larger is the incidence angle, the bigger is the missing part. This issue – that was reported to the software company – has been solved in forthcoming versions of the software⁸.



⁸ It has indeed been fixed with Envi5.0 SP3 (Service Pack 3): when modifying the pixel size of the orthoproduct with the option "Maintain map extent when pixel size changes", the output dimensions are recalculated, which was not the case with previous versions.

Figure 7: Issue encountered with Envi orthorectification module. Screenshot of Envi software. Some part of the input raw PAN (left) is missing in the corresponding orthorectified image (right), namely the South and East regions of the considered AOI.

6 External geometric quality control

The positional accuracy – also referred to as planimetric/horizontal accuracy – of the orthoimagery is expressed as the Root-Mean-Square Error (RMSE) of the geometric registration in Easting and Northing directions. The external quality control is done by measuring the misregistration of Independent Check Points (ICPs), in order to define the maximum permissible planimetric error $RMSE_{1D}$ ⁹. The results output by this procedure and the final

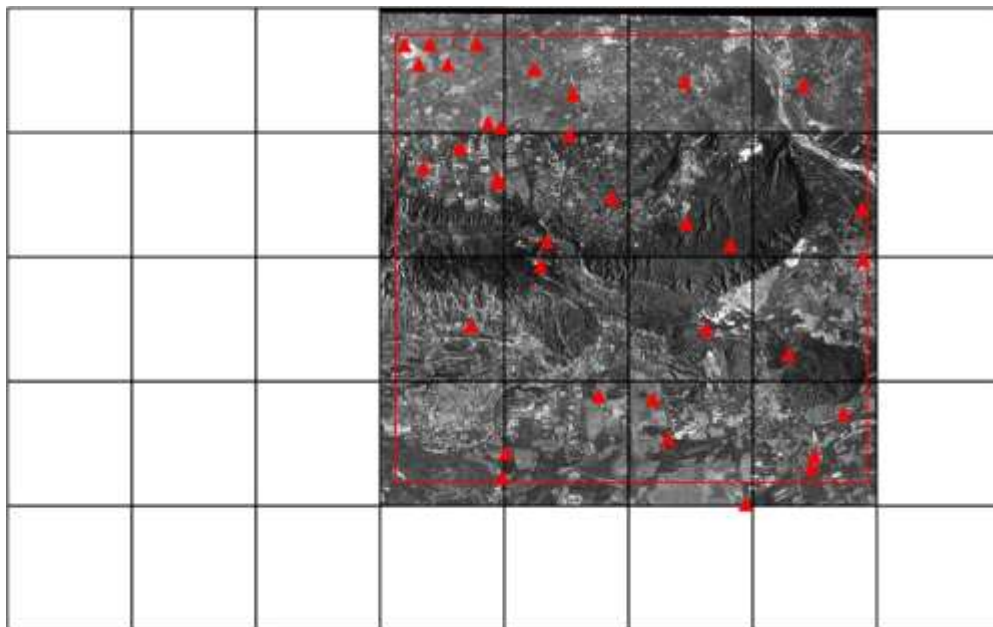


Figure 8: ICPs selection: ground and image identification. All validating ICPs are identified in the aerial images of the ADS40 dataset and located in PAN, MSP and PSH images through visual matching for error measurement.

validation are presented in this section.

⁹ See [5, Section 6.2] for a formal definition of the RMSE as a natural indicator of the overall geometric accuracy: $RMSE_{1D}$ represents the residual between the true georeferenced coordinates of the ICPs and their coordinates measured on the image.

6.1 Auxiliary validating data preparation

In order to evaluate the geometric characteristics of the orthoimagery produced using different input data and methodologies, it is enough to perform the EQC, that is to check its (geometric) accuracy on a set of ICPs:

- that were not included in the orthorectification model definition,
- whose ground coordinates are (known and) derived from other (possibly more accurate) source,
- whose image coordinates are (identified and) used as reference.

The accuracy is evaluated as the $RMSE_{1D}$ of the residuals (see next section) between the orthoimagery derived coordinates of this set of points and their true ground coordinates. This approach is referred to as the Hold-Out-Validation method in [8].

In that context, a set of ICPs is selected that will remain unchanged for all tested ortho products. In order to provide both spatially and statistically significant results, these ICPs are ideally [4, Section 12]:

- in sufficiently large number (so that *"the optimum distance between CPs is close to $1/10^{th}$ of the diagonal distance [of the AOI]"*), and

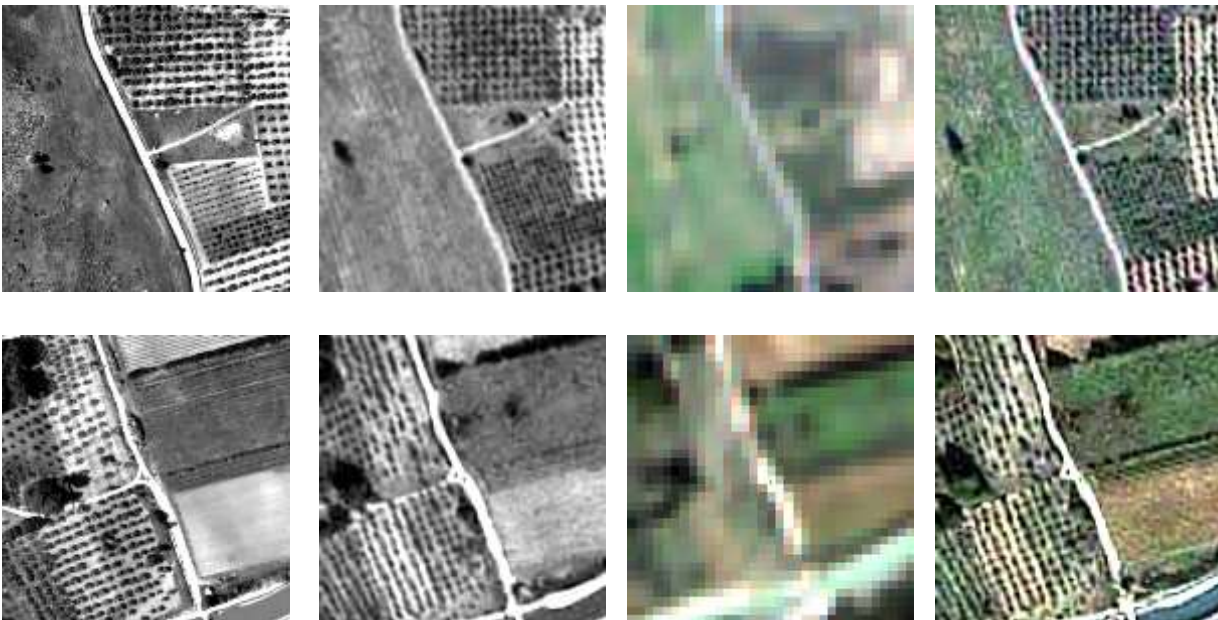


Figure 9: Examples of localisation in the orthoimagery of ICPs used for validation. From left to right: aerial image, corresponding PAN, MSP and PSH ortho products generated using PCI with 1, 3 and 4 GCPs resp., in this order. The identified/located ICP is displayed as a green 'plus' (+ symbol) in the centre of the different excerpts.

- evenly distributed and located across the entire image (so that "at least 20% of the points lay in each quarter [of the AOI]").

CPs are retrieved from ADS40 and Cartosat-2 datasets already described in Sections 4.3 and 5.1, and also Cartosat-1 and Formosat-2, considering the following positional accuracy $RMSE_{1D}$ of CPs:

- for Cartosat-1, $RMSE_{1D}[East] = 0.55m$ and $RMSE_{1D}[North] = 0.37cm$,
- for Formosat-2, $RMSE_{1D}[East] = 0.88m$ and $RMSE_{1D}[North] = 0.72m$.

In total, 35 ICPs are selected to evaluate the geometric accuracy of SPOT 4°, 22°, and 27°. However, as a consequence of the remark of Section 5.2 regarding 'missing parts' in Envi ortho products, only a subset of the available ICPs (28 instead of 35, still a relevant sample according to JRC guidelines [4]) was used to validate the data generated by this software. Following, the identification of ICPs is repeated over each ortho product. In practice, this operation is performed by the same operator as the one involved in the GCPs selection.

6.2 Results and discussion

The results of the evaluation of the various orthoimagery products considered for benchmarking (encompassing the test cases [3.i] to [3.v], see Table 2) are presented in Tables 3 to 6 and discussed in the following.

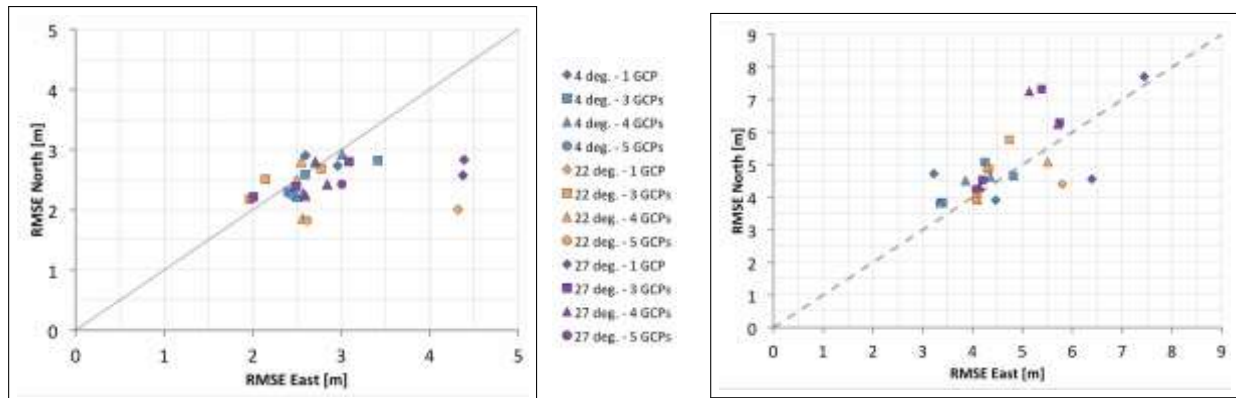


Figure 10: Overall graph representation of the $RMSE_{1D}$ error calculated in bundle ortho products. The $RMSEs$ measured over the ICPs selected by JRC in both PAN (panchromatic, left) and MSP (multispectral, right) orthoimages are displayed. Every single ortho product is shown as an entry marker – identified by the viewing angle of the primary input image (4°, 22° and 27°), and the number of GCPs used for orthorectification (1: •, 3: ◻, 4: ◻, or 5: ◻ GCPs) – whose coordinates in the graph represent the $RMSEs$ measured in both Easting/Northing directions (referred to as $RMSE_{1D}[East/North]$).

Overall results

A quick glance at the results presented in Figure 10 shows that as soon as $\#\{GCPs\} \geq 3$:

- over all PAN orthoimages and for all softwares, $RMSE_{1D} \leq 3.5m$ is achieved,
- over all MSP orthoimages generated using 'derived' GCPs, $RMSE_{1D} \leq 8m$ is achieved, and as well (see Table 7):
- over PSH orthoimages generated with PCI¹⁰, $RMSE_{1D} \leq 3m$ is achieved.

As for the directional error:

- the RMSE over PAN and PSH orthoimages is observed to be higher in Easting than in Northing direction.

Namely, in both cases, the $RMSE_{1D}$ over all ICPs is measured with values in the range $[1.5m, 3m]$ in Northing direction, and in the range $[2m, 4.5m]$ in Easting direction. On the contrary:

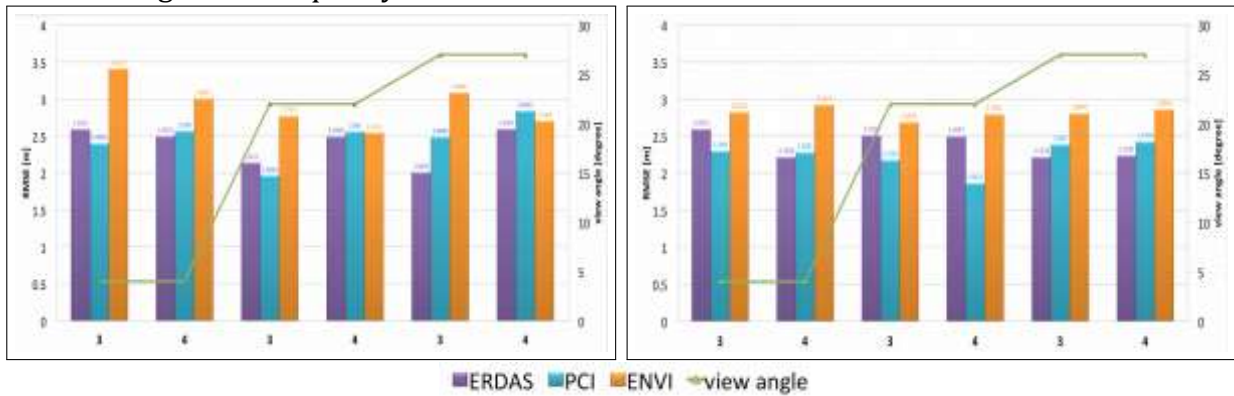
- the error measured in MSP orthoimages is sensibly higher in Northing (range $[3.5m, 8m]$) than in Easting (range $[3m, 7.5m]$) direction.

Notice however that such an anisotropic misregistration is not observed with one of the softwares used in the study, namely PCI, and significantly reduced with all other softwares as soon as $\#\{GCPs\} \geq 3$ in modeling the orthocorrection (see below).

		4	22	27					
		GCPs East North East North				East	North		
								#	
	3	2.4003	2.2983	1.9654	2.1761	2.4889	2.3887	[m]	
		[m]	[m]	[m]	[m]			[m]	
PCI									
	4	2.569	2.2801	2.562	1.8621	2.8431	2.4238		
Envi	3	3.4121	2.8229	2.7742	2.6876	3.0886	2.8044		
	4	3.0097	2.9221	2.5472	2.7965	2.7065	2.8606		
ERDAS	3	2.5937	2.5921	2.1421	2.5103	2.0095	2.2159		
	4	2.5015	2.2166	2.4938	2.4997	2.58967	2.2392		

(a) The RMSEs of the different available softwares are compared. The East (resp. North) columns store the $RMSE_{1D}[East]$ (resp. $RMSE_{1D}[North]$) errors measured over the different products as expressed in meters. For each PAN image (hence, per column, disregarding the number of GCPs employed), the highest and lowest errors observed in Easting and Northing directions using the available softwares are displayed as red and blue boxes resp.

¹⁰ For reminder, only PCI-generated PSH orthoimages are tested herein.



(b) The RMSEs of PAN orthoproducts generated using ERDAS, PCI and Envi softwares (Table 3a above), in both Easting (left) and Northing (right) directions, are represented as a function of the incidence angle (4°, 22° and 27° steps) and the number of GCPs (3 or 4) used.

Table 3: Planimetric RMSE_{1D} measurements on PAN orthoimagery: per software and per angle results for products [3.i]. The RMSEs in Easting and Northing directions estimated with all softwares, but only two GCPs configurations, are presented.

Analysis of bundle orthoproducts

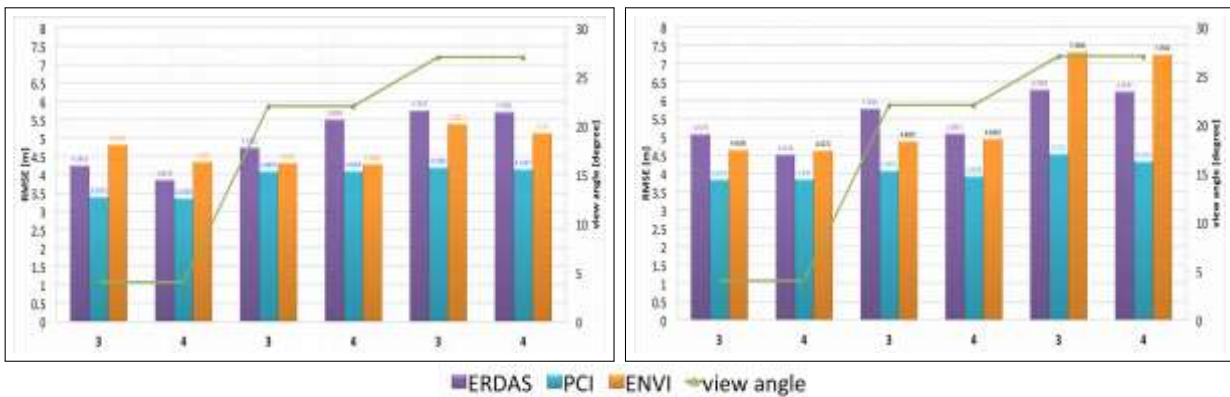
Tables 3 to 5 represent the sensitivity of the orthorectification of both PAN and MSP products w.r.t. various factors already mentioned earlier (see Section 3.1). A closer analysis of the RMSE_{1D} estimations calculated for the various softwares, angles and configurations enable to further evaluate the effect of those factors on the orthoimage accuracy, namely:

- the **software used for the implementation**; the configurations with 3 and 4 GCPs – as they are often used in orthorectification process – are considered for a thorough evaluation of the various software implementations in Tables 3a and 4a; the use of PCI and ERDAS softwares provide with the best outcomes for PAN orthorectification demonstrating, indeed, a RMSE_{1D} below 3m in both directions (in PCI case, this is also

		4°	22°	27°				#
		GCPs East North East North East North						
PCI	3	3.3973	3.8355	4.0893	4.0801	4.1965	4.5372	[m]
	4	3.3558	3.839	4.0964	3.9288	4.1467	4.3291	[m]
ERDAS	3	4.8163	4.6505	4.3202	4.8837	5.3851	7.3246	[m]
	4	3.3558	3.839	4.0964	3.9288	4.1467	4.3291	[m]

Envi		4	4.355	4.6272	4.2898	4.9459	5.137	7.2564
ERDAS	3	4.2453	5.0774	4.7361	5.7695	5.7437	6.2909	
	4	3.8573	4.5194	5.5069	5.0871	5.7061	6.2447	

(a) Ibid caption of Table 3a for MSP products.



(b) Ibid caption of Figure 3b for MSP products (left: Easting and right: Northing).

Table 4: Planimetric RMSE_{1D} measurements on MSP orthoimagery: per software and per angle results for products [3.i]. The ortho-products considered here are those generated using the so-called 'derived' GCPs, i.e. their locations is – namely – derived from their higher resolution positions defined in the coregistered PAN image. See caption of Table 3 for description, and similar results on PAN orthoimages.

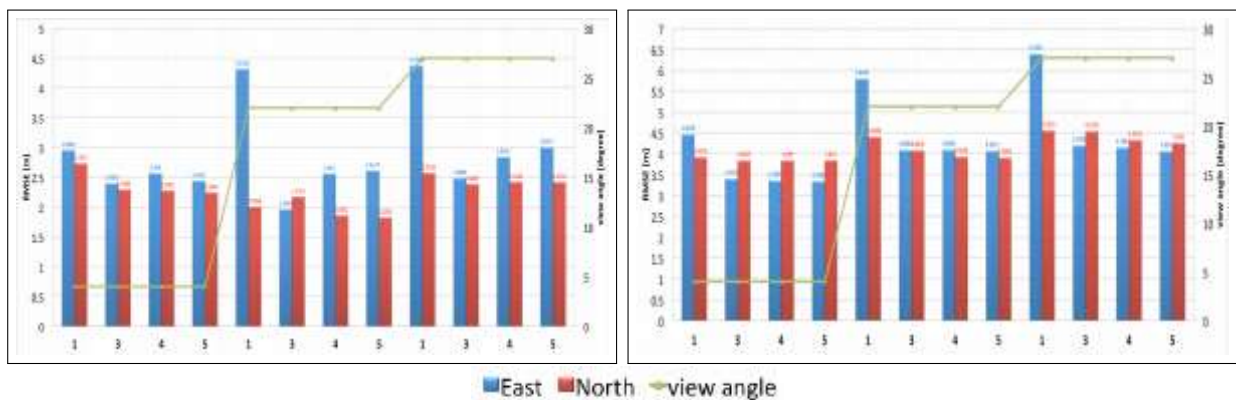
confirmed for #{GCPs} = 5 in Tables 5a); Envi results are similar in the Northing direction, and still reasonable in the Easting direction (RMSE_{1D} below 3.5m); over the MSP test case images considered in this study, PCI software outperforms both ERDAS and Envi softwares, as generated products present a RMSE_{1D} below 5m (hence, below the pixel size) in both directions; the latter two provide with orthoproducts whose misregistration is below 6m in Easting direction and below 8m in Northing direction;

- the **viewing (off-nadir) angle of the input image**; while the impact of the viewing angle on the accuracy of the PAN correction is not clear (no obvious correlation with the RMSE_{1D} error, see Figure 3b), as for MSP images, the error tend to increase with the angle so that the further-from-nadir image (27°) present the highest misregistration (see Figure 4b); closer-to-nadir images (4° and 22°) instead are registered with a RMSE_{1D} below 6m; this trend – resp., absence of trend – over MSP – resp., PAN – images seems verified through all the products generated with different configuration/number of GCPs in the Figure 5b, right – resp., left;

GCPs #

	off-nadir [angle]	1	3	4	5 bundle [m]	dir. [m]	[m]	[m]	[m]
4°	PAN			East	2.9603	2.4003	2.569	2.4431	
				North	2.7347	2.2983	2.2801	2.2466	
				2D	4.0301	3.3232	3.4349	3.319	
	MSP			East	4.4628	3.3973	3.3558	3.3389	
				North	3.9176	3.8355	3.839	3.841	
				2D	5.9384	5.1237	5.0989	5.0893	
22°	PAN			East	4.3194	1.9654	2.562	2.6137	
				North	2.0068	2.1761	1.8621	1.8285	
				2D	4.7628	2.9323	3.1672	3.1898	
	MSP			East	5.8006	4.0893	4.0964	4.0671	
				North	4.4048	4.0801	3.9288	3.9083	
				2D	7.2834	5.7767	5.6759	5.6405	
27°	PAN			East	4.3759	2.4889	2.8431	3.0077	
				North	2.5738	2.3887	2.4238	2.4232	
				2D	5.0767	3.4497	3.7361	3.8624	
	MSP			East	6.3932	4.1965	4.1467	4.061	
				North	4.5559	4.5372	4.3291	4.256	
				2D	7.8504	6.1803	5.9947	5.8826	

(a) The $RMSE_{1D}$ and $RMSE_{2D}$ measured over various PCI-generated orthoproducts are compared. The East (resp. North and 2D) rows store the $RMSE_{1D}[East]$ (resp. $RMSE_{1D}[North]$ and $RMSE_{2D}$) errors expressed in meters. The highest and lowest errors observed independently of the input configuration (number of GCPs used, hence per row) are displayed as red and blue boxes resp.

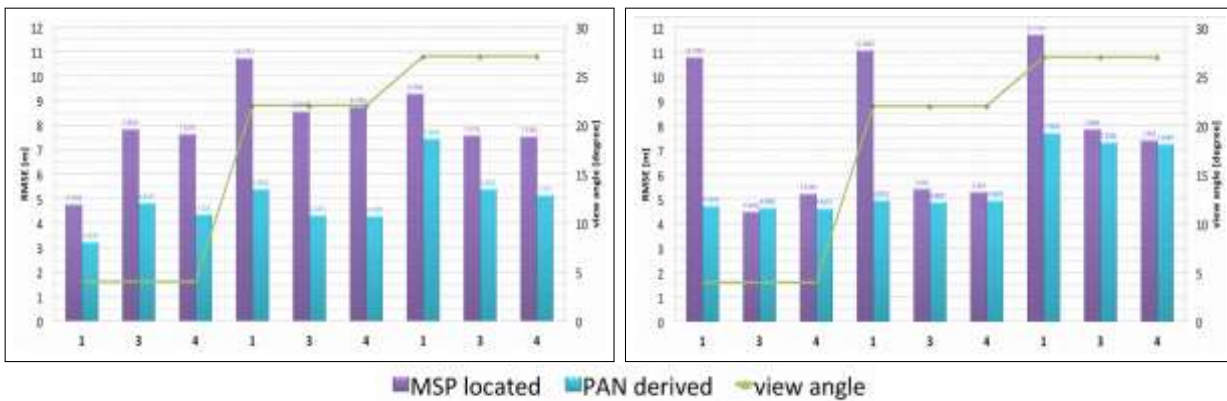


(b) The $RMSE_{1D}$ measured in PAN (left) and MSP (right) orthoproducts (Table 5a above) are represented in both Easting and Northing directions, as a function of the incidence angle (4°, 22° and 27°, see Figure 3b) and the number of GCPs (1, 3, 4 or 5) used.

Table 5: **Planimetric RMSE_{1D} and RMSE_{2D} measurements on PAN and MSP orthoimagery: per GCPs configuration results for products [3.iii].** The RMSEs in Easting and Northing directions of the orthoproducts generated using PCI software only are presented for all possible input configurations.

GCPs type		4°		22°		27°	
		East	North	East	North	East	North
#		[m]	[m]	[m]	[m]	[m]	[m]
1	located	4.7588	10.7985	10.7372	11.0845	9.2786	11.7114
	derived	3.2245	4.7245	5.3902	4.9552	7.4448	7.7052
3	located	7.8353	4.4836	8.5579	5.426	7.5713	7.8604
	derived	4.8163	4.6505	4.3202	4.8837	5.3851	7.3246
4	located	7.6279	5.2248	8.7399	5.294	7.5386	7.404
	derived	4.355	4.6272	4.2898	4.9459	5.137	7.2564

(a) The RMSEs measured in Envi MSP orthoproducts generated using either 'located' or 'derived' GCPs are compared (see Table 3a for a description of East and North columns). For each angle (hence, per column), the highest and lowest errors observed independently of the number and the nature of the GCPs in either Easting or Northing directions are displayed as red and blue boxes resp.



(b) The RMSEs measured using either the 'located' (in MSP) or 'derived' (from PAN) approach (Table 6a above) are represented in both Easting (left) and Northing (right) directions, as a function of the incidence angle (4°, 22° and 27°, see Figure 3b) and the number of GCPs (1, 3 or 4) used.

Table 6: **Representation of planimetric RMSE_{1D} error on MSP orthoimagery using either derived or located GCPs: per GCP localisation/type results for products [3.v].** The RMSEs in Easting and Northing directions of the orthoproducts generated using Envi software only are presented for different input configurations with GCPs whose locations is either defined ('located') directly in the MSP image, or 'derived' from the higher resolution positions in the corresponding PAN image (see Table 10 in Annex A).

- the **number (and distribution) of GCPs used for modeling**; as soon as #{GCPs} ≥ 3, the increase of GCPs does not seem to improve the geolocation accuracy,

independently of the software used (see Tables 3 and 4): orthorectifying with 3, 4 GCPs prove to generate orthoproducts with similar degree of misregistration; this is confirmed in Table 5a (left and right) when considering PCI only and looking at the results produced with 5 GCPs as well; there are no significant improvements however when using more GCPs: this could be explained, in our case, by the accuracy of the input ancillary data (see Section 4.3) that may introduce errors in the localisation of the GCPs; the products generated 1 GCP present the highest error in misregistration and should be avoided as such, especially when dealing with far-from-nadir images (22° and 27°, see Figure 5b).

Another relevant analysis aims at questioning whether one should fully exploit the spatial information available in the PAN images – commercialised with the bundle product – when correcting MSP images, namely deciding about:

- the **nature of the GCPs used for modeling**; all previously described MSP products were generated using so-called '*derived*' GCPs, *i.e.* GCPs whose locations have been prior defined in the PAN image then downsampled to the MSP grid (see Section 3.2); while the reported RMSE_{1D} are generally below the pixel size (*cf.* previous items), the interest of using such approach compared to a '*located*' one, where GCPs locations are estimated directly in the MSP images, can be understood from Table 6; using indeed '*located*' GCPs enables to produce orthoproducts with in general higher misregistration error, especially in Easting direction in the present case (around 2m more, see Figure 6b, left).

Analysis of pansharpened orthoproducts

The results of the analysis of the PSH orthoproducts are presented in Tables 7. In particular, the in-house Reference3D product commercialised by Astrium can be compared to the products generated using ancillary data with PCI COTS software. Likewise previous analysis, it is possible at that stage to evaluate the influence of some of the abovementioned factors on the positional accuracy of the output products:

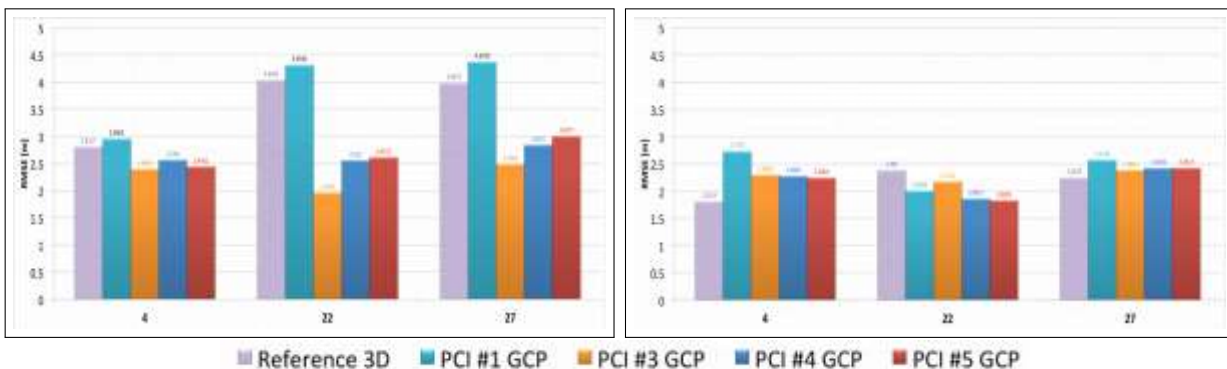
- the Reference3D orthoimages show good registration, below 4m in both directions and for all viewing angles – therefore, verifying the absolute planimetric accuracy (10m CE90) claimed by the image provider; with a close-to-nadir image (4°), this value gets even below 3m; hence, the geometric quality of this product, generated without any external GCP, is comparable to that of the product generated using 1 GCP with PCI (see Table 7a);
- if one aims at incorporating additional information from available modeling GCPs, the PCI-generated orthoimages provide with a relatively high positional accuracy as soon

External quality control of SPOT6 orthoimagery

as $\#\{GCPs\} \geq 3$, as the estimated $RMSE_{1D}$ reaches values below 3m – hence, twice the pixel size – for all viewing angles (see Table 7a); indeed, among the tested

		4°	22°	27°			
GCPs East North East North East North							
	#	[m]	[m]	[m]	[m]	[m]	[m]
Reference3D		2.8137	1.8119	4.0435	2.389	3.9877	2.2478
	1	2.9603	2.7347	4.3194	2.0068	4.3759	2.5738
	3	2.4003	2.2983	1.9654	2.1761	2.4889	2.3887
PCI							
	4	2.569	2.2801	2.562	1.8621	2.8431	2.4238
	5	2.4431	2.2466	2.6137	1.8285	3.0077	2.4232

(a) The RMSEs measured in Reference3D and PCI orthoproducts are compared (see Table 3b for a description of East and North columns). For each angle (hence, per column), the highest and lowest errors observed independently of the considered product in either Easting or Northing directions are displayed as red and blue boxes resp.



(b) The RMSEs of the different available products (Reference3d and PCI with 1, 3, 4 and 5 GCPs: Table 7a above) are represented in both Easting (left) and Northing (right) directions, as a function of the incidence angle (4°, 22° and 27°).

Table 7: Planimetric $RMSE_{1D}$ measurements on PSH (pansharpended) orthoimagery: per angle results for products [3.ii] and [3.iv]. The RMSEs measured in Easting and Northing directions in the (so-called) Reference3D orthoimages distributed by Astrium, as well as those generated using PCI and different input GCPs configurations, are presented.

products, the generated PSH orthoimages¹¹ show very high spatial correlation with their corresponding PAN orthoimage so that the localisations of ICPs in both products were

¹¹ Notice that the pansharpending process implemented in PCI is fully integrated in the orthocorrection workflow within the OrthoEngine module of the software, and applied before the geometric correction; the

identical to a precision of a tenth of a pixel (0.15m); in addition, the results show very little, to null, influence from the viewing angle and the number of GCPs used on the accuracy (see Figure 7b).

7 Conclusion

The main objective of the study presented in this document was to assess whether SPOT6 sensor can be qualified for use in CAP checks (CwRS and LPIS). The **External Quality Control assessing SPOT6 orthoimagery from a geometric perspective** has been performed in accordance with the standard methodology and guideline enounced by JRC [4]. For that purpose, a benchmarking aiming at both evaluating the positional accuracy of SPOT6 orthoimagery, and measuring the influence of different factors (viewing angle, number of GCPs, software platform) on the accuracy was operated.

Following the results of this benchmarking, it is asserted that the sensor fulfills the following geometric specifications for use as VHR back-up ortho-products in the CAP:

- **a planimetric accuracy $RMSE_{1D} \leq 3.5m$ is reached on PAN orthoimages, as soon as a relevant number of modeling GCPs is used** (in this study, $\#\{GCPs\} \geq 3$ provides satisfactory results),
- **$RMSE_{1D} \leq 4m$ is fulfilled by Reference3D PSH orthoimages** (generated without any external GCP) and goes below 3m when close-to-nadir image is considered,

in both Easting and Northing directions and for all considered COTS softwares. In particular, the Reference3D PSH orthoproducts prove to be an interesting alternative to use as backup VHR imagery for the CAP checks, especially for close-to-nadir acquisitions, when positional data is not available. In addition, in the case the users may want to apply their own pansharpening of SPOT6 primary products and GCPs are available for orthocorrection, they can generate PSH orthoimages – instead of using PSHReference3D products directly – for which it is shown with one software (PCI) that:

- $RMSE_{1D} \leq 3m$ can be reached on PSH orthoimages with $\#\{GCPs\} \geq 3$.

Similarly, the specifications for the HR products are as follows:

- **$RMSE_{1D} \leq 8m$ is reached on MSP orthoimages as soon as $\#\{GCPs\} \geq 3$.**

Hence, the "thumb rule" $1.5 \times GSD$ generally observed in HR imagery is also fulfilled by SPOT6 products. In that case, it appears that the quality of the orthocorrection benefits from the derived estimation of the modeling GCPs positions in the PAN (primary) image, instead of a direct localisation in the MSP image. Therefore, it is recommended to the users to retrieve the

specific algorithm used for pansharpening is derived from the fusion approach of [16] which has demonstrated good results with VHR data (*e.g.* WorldView-2). On the contrary, other COTS platforms like Envi or ERDAS leave the choice of the pansharpening algorithm to the user and implement it as separate modules.

GCPs locations in MSP images through a simple grid downsampling of their locations in the corresponding PAN images, so as to fully exploit the high-resolution spatial information made available in the commercialised bundle products. In this context, the Reference3DPSH orthoimagery (see abovementioned results) can be again regarded – from a geometric perspective, and provided further testing of their radiometric accuracy – as a possible alternative in HR controls (*e.g.* to help in visual interpretation).

Finally, it also arises from the present study that the error in misregistration was reduced employing specific given softwares:

- $RMSE_{1D} \leq 3m$ (*i.e.*, $2 \times GSD$) is reached on PAN orthoimages generated with either ERDAS or PCI,

7. Conclusion

- $\text{RMSE}_{10} \leq 6m$ (*i.e.*, the GSD) is fulfilled by MSPPCI-generated orthoimages,






again, when using a relevant number of modeling GCPs. Hence, it is believed that further focus could be given to the various configurations and/or implementations in the different COTS softwares to reach similar results with all of them. Therefore, this validation should be the subject of additional testing procedure.

Annex A: description of the GCPs

We provide here some information regarding the selected GCPs employed in orthorectification (see Section 4.3) as to locate them in – primary and ortho – images.

#	ID	ground position [m]		height [m]	
		North	East	ellipsoidal	orthometric
1	110037	4842537,189	657075,557	225,567	175,497
2	G7010	4851674,942	648932,1747	N/A	80,709
3	110051	4850624,772	667097,535	135,407	85,157
4	110056	4837771,413	664787,963	137,112	87,074
5	110031	4840147,739	652245,853	92,137	42,117

Table 8: Ground position and height of selected GCPs. In-situ measured GPS (North, East) coordinates in EPSG 32631 reference system and respective heights.

#	ID	source	screen shot	ground camera shot
1	110037	ADS40		
2	G7010	Cartosat-2		
3	110051	ADS40		

7. Conclusion

4	110056	ADS40		
---	--------	-------	---	--

5	110031	ADS40		
---	--------	-------	---	---

Table 9: GCPs selection over Mausanne site. GCPs from 2 different datasets are selected and positioned on the primary imagery based on the available visual information (ground camera shots and aerial image screenshots).

GCP #	bundle	type	image location [pixels]					
			4°		22°		27°	
			X	Y	X	Y	X	Y
1	PAN	located	5395,5	7774,2	4733,5	7354,9	4557,4	7235,9
		derived	1348,9	1943,6	1183,4	1838,7	1139,4	1809
2	MS	located	1349,3	1945,3	1184,7	1836,7	1139,9	1807,4
		located	340,9	1828,8	276,2	2042,7	261,8	1604,2
		derived	85,2	457,2	69,1	510,7	65,5	401,1
3	MS	located	84,4	457,3	68,5	510,4	65,2	400,4
		located	11869,8	2743,7	10553,2	2344,4	10162,8	3545,4
		derived	2967,5	685,9	2638,3	586,1	2540,7	886,4
4	MS	located	2966,7	686,3	2636,4	585,1	2539,3	885,1
		located	10210,7	10920,3	9082,8	10080,4	8741,8	10408,9
		derived	2552,7	2730,1	2270,7	2520,1	2185,5	2602,2
5	MS	located	2553,8	2730,6	2271,6	2519,3	2186,1	2602,5
		located	2283,4	9233,9	1999,3	8878,7	1925,1	8155,6
		derived	570,9	2308,5	499,8	2219,7	481,3	2038,9
5	MS	located	571,7	2306,9	499,3	2220,4	480,3	2040,2

Table 10: Localisation of selected GCPs in images. (column,row) image coordinates (X,Y) in 4°, 22° and 27° are identified by a human operator (1 digit precision, i.e. a tenth of a pixel) in PAN and MSP ('native' line) images. In addition, (X,Y) coordinates in MSP images are automatically deduced from the PAN coordinates ('derived' line) through simple downsampling, i.e. (X,Y) coordinates are divided by 4 and rounded (to a 1/10 of a pixel). The average error between 'located' and 'derived' locations is around 1 pixel (hence, 6m).

References

- [1] JRC IES, *Common technical specifications for the 2012 CwRS campaign*, 2012, available at <http://mars.jrc.ec.europa.eu/mars/content/download/2313/12060/file/CwRS-2.pdf>.
- [2] JRC IES, *Orthoimage technical specifications for the purpose of LPIS*, wiki available at http://marswiki.jrc.ec.europa.eu/wikicap/index.php/Orthoimage_technical_specifications_for_the_purpose_of_LPIS.
- [3] JRC IES, *Accuracy of the orthoimagery used in CwRS*, wiki available at http://marswiki.jrc.ec.europa.eu/wikicap/index.php/Accuracy_of_the_orthoimagery_used_in_CwRS.
- [4] D. Kapnias, P. Milenov, and S. Kay, "Guidelines for best practice and quality checking of ortho imagery", Tech. Rep. 48904, JRC IPSC, 2008, available at http://mars.jrc.ec.europa.eu/mars/content/download/1231/7140/file/Orthoguidelines_v3_final.pdf; wiki available at http://marswiki.jrc.ec.europa.eu/wikicap/index.php/Guidelines_for_Best_Practice_and_Quality_Checking_of_Ortho_Imagery.
- [5] J. Grazzini, S. Lemajic, and P.J. Astrand, "External quality control of Pléiades orthoimagery – Part I: Geometric benchmarking and validation of Pléiades-1A orthorectified data acquired over Maussane test site", Tech. Rep. 82308, JRC IES, 2013.
- [6] J.A. Gutierrez and B.S.R. Armstrong, *Precision Landmark Location for Machine Vision and Photogrammetry – Finding and Achieving the Maximum Possible Accuracy*, Springer-Verlag, London (UK), 2008.
- [7] W. Linder, *Digital Photogrammetry – A Practical Course*, Springer, 2009, 3rd edition.
- [8] P.J. Astrand, M. Bongiorno, M. Crespi, F. Fratarcangeli, J. Nowak Da Costa, F. Pieralice, and A. Walczynska, "The potential of WorldView-2 for ortho-image production within the "Control with Remote Sensing Programme" of the European Commission", *International Journal of Applied Earth Observation and Geoinformation*, vol. 19, pp. 335–347, 2012.
- [9] A. Walczynska and J. Nowak Da Costa, "THEOS geometric image quality testing – Initial findings", Tech. Rep. 61992, JRC IPSC, 2010, available at <http://publications.jrc.ec.europa.eu/repository/bitstream/111111111/15348/1/lbna24655enn.pdf>.
- [10] J. Nowak Da Costa and A. Walczynska, "Geometric quality testing of the Kompsat-2 image data acquired over the JRC Maussane test site using ERDAS References

LPS and PCI Geomatics remote sensing softwares”, Tech. Rep. 60285, JRC IPSC, 2010, available at <http://publications.jrc.ec.europa.eu/repository/bitstream/111111111/15039/1/lbna24542enn.pdf>.

- [11] J. Nowak Da Costa and A. Walczyn´ska, “Geometric quality testing of the WorldView-2 image data acquired over the JRC Maussane test site using ERDAS LPS, PCI Geomatics and Keystone digital photogrammetry software packages – Initial findings with annex”, Tech. Rep. 64624, JRC IPSC, 2011, available at http://publications.jrc.ec.europa.eu/repository/bitstream/111111111/22790/1/jrc60424_lb-nb-24525_en-c_print_ver.pdf.
- [12] J. Nowak Da Costa and P.A. Tokarczyk, “Maussane test site auxiliary data: existing datasets of the Ground Control Points”, Tech. Rep. 56257, JRC IPSC, 2010.
- [13] C. Lucau and J. Nowak Da Costa, “Maussane GPS field campaign: methodology and results”, Tech. Rep. 56280, JRC IPSC, 2009, available at http://publications.jrc.ec.europa.eu/repository/bitstream/111111111/14588/1/pubsy_jrc56280_fmp11259_sci-tech_report_cl_jn_mauss-10-2009.pdf.
- [14] J. Nowak Da Costa and P.A. Tokarczyk, “The GCP dataset based on the Leica Geosystems ADS40 digital airborne camera orthoimagery”, Tech. Rep. 56254, JRC IPSC, 2010.
- [15] T. Toutin, “Geometric processing of remote sensing images: models, algorithms and methods”, *International Journal of Remote Sensing*, vol. 10, pp. 1893–1924, 2004.
- [16] Y. Zhang, “Understanding image fusion”, *Photogrammetric Engineering and Remote Sensing*, vol. 70, no. 6, pp. 657–661, 2004.

List of Figures

1	Examples of pansharpened SPOT6 acquisitions in Southern France.	7
2	Multispectral acquisitions over Maussane test site and corresponding footprints.	10
3	Pansharpened orthoimagery over Maussane test site.	11
4	Maussane test site and related available JRC ancillary data: DEM and CPs.	12
5	Available JRC ancillary data over Maussane AOI: DEM.	14
6	GCPs identification and configuration.	15
a	GCPs identification in ADS40 aerial images.	15
b	GCPs selection and spatial configurations in primary raw images. . .	15
7	Issue encountered with Envi orthorectification module.	16
8	ICPs selection: ground and image identification.	17
9	Examples of Localisation over the ortho-products of the ICPs used for validation.	18
10	Overall graph representation of RMSE _{1D} error on ortho bundle products. . .	19

List of Tables

1	Main characteristics of SPOT system.	6
2	Benchmarking configurations.	8
3	Planimetric 1D RMSEs measurements on panchromatic orthoimagery.	20
a	Comparison of $RMSE_{1D}$: per software and per angle.	20
b	Graph representation of $RMSE_{1D}$: per software and per angle.	20
4	Planimetric 1D RMSEs measurements on multispectral orthoimagery.	21
a	Comparison of $RMSE_{1D}$: per software and per angle.	21
b	Graph representation of $RMSE_{1D}$: per software and per angle.	21
5	Planimetric 1D and 2D RMSEs measurements on panchromatic and multi-spectral orthoimagery.	22
a	Comparison of $RMSE_{1D}$ and $RMSE_{2D}$: per GCPs configuration. ...	22
b	Graph representation of $RMSE_{1D}$: per GCPs configuration.	22
6	Planimetric 1D RMSEs on ortho multispectral products using either derived or located GCPs.	23
a	Comparison of $RMSE_{1D}$: per GCP localisation/type.	23
b	Graph representation of $RMSE_{1D}$: per GCP localisation/type.	23
7	Planimetric 1D RMSEs measurements on pansharpened orthoimagery.	25
a	Comparison of $RMSE_{1D}$: per angle.	25
b	Graph representation of $RMSE_{1D}$: per angle.	25
8	Ground position and height of selected GCPs.	28
9	GCPs selection over Mausanne site.	29
10	Localisation of selected GCPs in images.	29

European Commission
EUR 26103 – Joint Research Centre – Institute for Environment and Sustainability

Title: External quality control of SPOT6 orthoimagery - Geometric benchmarking over Maussane test site for positional accuracy assessment

Authors: J. Grazzini and P. Astrand

Luxembourg: Publications Office of the European Union

2013 – 37 pp. – 21.0 x 29.7 cm

EUR – Scientific and Technical Research series – ISSN 1831-9424

ISBN 978-92-79-32543-4

DOI: 10.2788/98290

Abstract

The main objective of the present study is to assess whether SPOT6 sensor can be qualified for Control with Remote Sensing programmes, specifically in Common Agriculture Policy (CAP) Controls image acquisition campaign. The benchmarking presented herein aims at:

- evaluating the usability of SPOT6 for the CAP checks through an estimation of its geometric (positional) accuracy, • measuring the influence of different factors (viewing angle, number of GCPs, software implementation) on the abovementioned accuracy.

For that purpose, the External Quality Control of SPOT6 orthoimagery conforms to the standard method developed by JRC and follows a procedure already adopted in the validation of previous high and very-high resolution products.

As the Commission's in-house science service, the Joint Research Centre's mission is to provide EU policies with independent, evidence-based scientific and technical support throughout the whole policy cycle.

Working in close cooperation with policy Directorates-General, the JRC addresses key societal challenges while stimulating innovation through developing new standards, methods and tools, and sharing and transferring its know-how to the Member States and international community.

Key policy areas include: environment and climate change; energy and transport; agriculture and food security; health and consumer protection; information society and digital agenda; safety and security including nuclear; all supported through a cross-cutting and multidisciplinary approach.

